TEMPERATURE DEPENDENCE OF PHOTOVOLTAGES GENERATED BY BACTERIORHODOPSIN

G. W. RAYFIELD
Department of Physics, University of Oregon, Eugene, Oregon 97403

ABSTRACT The temperature dependence of the photovoltage developed by a model membrane containing bacteriorhodopsin (BR) is studied. The model membrane is formed by first coating a thin Teflon sheet with lipid and then fusing BR vesicles to it. The time course of the photoresponse is resolved down to 1 μs. The photoresponse is taken to be a sum of exponentials. Exponential time constants and amplitudes are determined by an analysis of the photoresponse with a photovoltage vs. log time plot, correlation filter, and nonlinear least-squares routine. The photovoltage is taken to be the sum of three exponentials but only two of the three time constants are resolved. Both are temperature dependent and indicate a thermally activated transport process. The corresponding activation energies are 55 kJ/mol and 62 kJ/mol. Since the photovoltage is proportional to charge times displacement the corresponding charge displacements are 11 and 34 Å asssuming a total displacement of 45 Å. The remaining exponential term corresponds to a small negative transient in the photovoltage that has a rise time <1 μs even at −20°C. The calculated charge displacement is estimated to be <2 Å.

INTRODUCTION

Bacteriorhodopsin (BR) is a light-activated proton pumping protein found in the cell wall of *Halobacterium halobium*. There is considerable detailed information now available about the structure, photochemistry, and nature of the chromophore (retinal) in the protein (1, 2). However, experimental data relevant to the light-activated charge movements in the protein are not extensive and are quantitatively inconsistent. These inconsistencies have been discussed in the literature (3, 4, 5).

Even though data derived from photoresponse measurements are not in absolute agreement, a general framework that describes the data can be constructed: Three different time domains exist in the photoresponse. First there is a fast (negative) transient ($\tau_1 < 1$ μs) followed by a slower (positive) component (20 μs $< \tau_2 <$ 90 μs) followed finally by a very slow (positive) component with τ_3 greater than several milliseconds. This scheme describes the data of Drachev et al. (6) using BR in lecithin impregnated filters, Trissl (4) using BR in monolayer films, and Ehrenberg et al. (3) using a fast responding dye with BR vesicles. Fahr et al. (7) report a value (τ = 1 ms) for the slowest component that is probably unreliable due to the technique used in measuring the photoresponse (voltage clamp) (8) and charging effects associated with signal averaging (9). Varo and Keszthelyi (10) used dried purple membrane for their studies, which increases τ relative to purple membrane bathed by salt solutions. Keszthelyi and Ormos (11) investigated the photoresponse from purple membrane fragments suspended in triple distilled water, which among other difficulties, caused complications due to the presence of the 0 intermediate in low ionic strength solutions.

Photovoltages measure the product of charge times displacement (4, 5, 7, 11) so that the amplitude of each component of the photoresponse can be interpreted as being proportional to a charge displacement. The implication of the assumptions involved in this interpretation has been discussed by Nagle and Tristram-Nagle (12) with respect to possible models for the pump. Estimates of the charge displacement ratio for the second component to the third component range from 0.1 (11) to 0.3 (6) or 0.4 (4) except for the work of Fahr et al. (7) where the ratio is estimated to be ~10. This later value is suspect due to inherent difficulties they experienced in resolving the slow component of the photoresponse.

A measurement of the photoresponse at different temperatures indicates first of all whether or not a thermally activated process could be involved in the pumping mechanism and second what activation energy would be involved. The temperature dependence of the photoresponse has been investigated by Drachev et al. (6) and they report a barrier height of 67 kJ/mol for both the second and third components. No temperature dependence of the time constant is reported for the first process. Fahr et al. (7) report a barrier height of 41 kJ/mol for the first process, from 49–56 kJ/mol for the second, and 39 kJ/mol for the third, which is again unreliable for the reasons mentioned above. A relatively long time constant of 9 μs is reported for the first component of the photoresponse at 0°C.

In preceding work (5, 9) it was shown that a sensitive, rugged, and simple photoactive membrane containing BR can be formed by fusing BR vesicles to a very thin Teflon sheet. An analysis of the photoinduced electrical signal was

presented that relates these signals to discrete charge displacements within the membrane. The time resolution of the membrane generated photocurrents was limited to ~60 μs and only room temperature measurements were made.

The work described here is concerned with a measurement of photovoltages rather than photocurrents, which allows an extension of the time resolution to 1 μs. The temperature dependence of the photoresponse was studied from 0 to 40°C. Time constants were derived from the data using several different techniques: a plot of photovoltage vs. log time, a correlation filter technique, and nonlinear least-square curve fitting. Barrier heights for the thermally activated charge displacements were obtained from the temperature dependence of the photovoltage.

MATERIALS AND METHODS

Except for a few minor modifications, the photoactive membrane was formed as previously described (5). A brief summary of the procedure is given below and details may be found in the earlier publication. BR vesicles were fused onto a thin Teflon sheet that was precoated with a thin lipid layer. The Teflon sheet or septum separates two black Teflon chambers filled with electrolyte. Ag-AgCl electrodes are contained in separate light shielded compartments and are electrically connected to the bathing (electrolyte) solutions by thin electrolyte-filled channels. The bathing solutions are 100 mM NaCl with 5 mM $CaCl_2$ and are buffered to pH 7 with 5 mM pipes. BR was prepared from strain JW-3 of *Halobacterium halobium* following Becher and Cassium (13).

The Teflon cell with the photoactive membrane was mounted in an aluminum box, which was held at constant temperature by circulating water through it from a refrigerated bath (Neslab RTE-4DD; Neslab Instruments, Inc., Portsmouth, NH). The aluminum box was in turn mounted in a sealed Plexiglas box for thermal and vapor insulation. The chemical dye laser (model DL-2100A; Phase-R Co., New Durham, NH) used to excite the membrane was the same as that used in the earlier work (5). Rhodamine 590 dye was used and the laser was operated at 590 nm.

In the previous work (5) a current-to-voltage converter was used to detect the transient movement of charge when photoactivation occurs. As Huebner et al. (8) have noted, it is difficult to reduce the rise time of this type of instrumentation to less than ~10 μs and still maintain a good signal-to-noise ratio. The finite rise time of the electrometer can be corrected for to some extent by the techniques of linear system analysis (Laplace transforms). A better approach, however, is to measure photovoltages (8). The direct current (DC) output impedance of the experimental cell is infinite and this requires an input shunt resistance for the voltmeter to compensate the input bias current of the operational amplifier used in the voltmeter. We have constructed two voltmeters. One of the instruments has a frequency response of 10 MHz and an input impedance of 10^9 Ω, which, when the capacitance of the membrane (300 pF) is considered, limits the total measuring time to <100 ms. The other voltmeter has a frequency response of 1 MHz but an input impedance of 10^{11} Ω, which increases the RC (circuit) relaxation time constant for the instrument to 30 s. The relaxation of the photovoltage is, therefore, due primarily to backleakage of protons within the membrane. The technique used to form the photoactive membrane (5) produced very tight membranes so that distortion of the photoresponse due to relaxation of the induced photovoltage was minimal. A more complete discussion of a very similar problem has been given by Trissl (14).

The output from the voltmeter is connected to a Nicolet 4094 digital oscilloscope (Nicolet Scientific Corp., Northvale, NJ). This instrument has a vertical resolution of 12 bits with a maximum digitizing rate of 2 MHz. The instrument can store a maximum of 16,000 points in a single sweep. The analogue bandwidth is 1 MHz and this is the limiting factor in our time resolution (the laser pulse width is ~300 ns). Data from the oscilloscope (Nicolet Scientific Corp.) is fed to an IBM-PC computer for data processing (IBM Instruments, Inc., IBM Corp., Danbury, CT). A PIN photodiode triggered by the laser flash was used to provide a fast stable trigger for the oscilloscope (Nicolet Scientific Corp.).

RESULTS

Fig. 1 shows a photovoltage vs. log time isotherm. Data were taken at a temperature of 20°C. The curve is a composite of two photoresponse data sets, one taken at 0.5 μs/point and the other taken at 20 μs/point. This was necessary because of the extreme time span that had to be covered. Each data set contained 16,000 data points and they were joined at 1 ms to form the composite curve. The peak photovoltage for this curve was 36 mV and was normalized to 1. Using the relation $V_{peak} - Nq\delta x/\epsilon A$ (5) it was estimated that 1% of the membrane surface is covered by protein and overlapping of the purple membrane sheets was, therefore, negligible.

The shape of the photoresponse was unchanged when a 7.8% transmission neutral density filter was inserted in front of the actinic light flash. The peak photovoltage decreased only by a factor of 2.0. Thus, the full actinic light flash was strong enough to essentially saturate the photoresponse.

Signal averaging was not used since it led to membrane charging, which altered the kinetics of the photovoltage (5). Several minutes were allowed between even single laser flashes to insure that the membrane was fully relaxed. Within certain approximations (5), the photoresponse may be written as a sum of exponentials

$$V(t) = C^{-1} \int i\,dt = \Sigma A_i [1 - \exp(t/\tau_i)].$$

A_i is proportional to the number of charges and to the distance of charge movement associated with the ith event. τ_i is the decay time associated with the ith event.

The advantage of an amplitude vs. log time plot where a sum of exponentials is involved have been discussed by Nagle (15). Following this protocol three regions are clearly identified in Fig. 1: a fast initial negative photovoltage (labeled 1) followed by two points of inflection (labeled 2 and 3). The initial negative photovoltage (1) represents an unresolved component of small (negative) amplitude. Points of inflection (at 2 and 3) give estimates of the other time constants in the photoresponse. Slopes at the points of inflection are proportional to the corresponding amplitude of these components. Thus the time constant of the second event lies between 20 and 60 μs while the third time constant lies between 20 and 40 ms. The ratio of the amplitudes for the second and third events is 3.

A correlation filter technique (10) was also used to extract decay times from the time dependence of the photoresponse curve. Briefly the method consists of transferring the digitized photovoltage signal stored in the oscilloscope to a data array in the IBM PC computer. Two

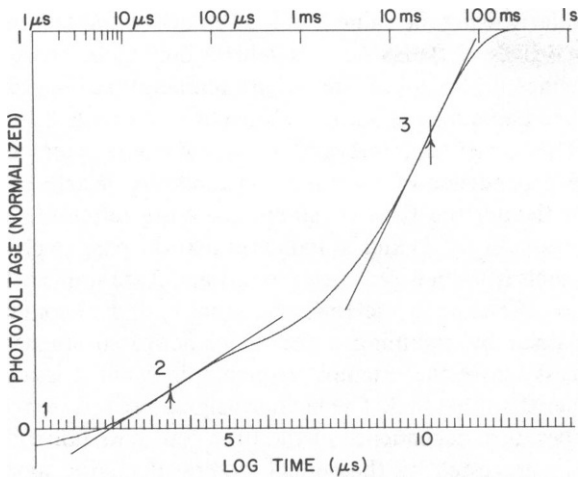

FIGURE 1 A typical photovoltage (normalized) vs. log time isotherm is shown at 20°C. Three components (labeled *1*, *2*, and *3*) of the photoresponse are identified. Points of inflection at *2* and *3* indicate two of the time constants involved. Arrows indicate time constants found using a correlation filter on the data.

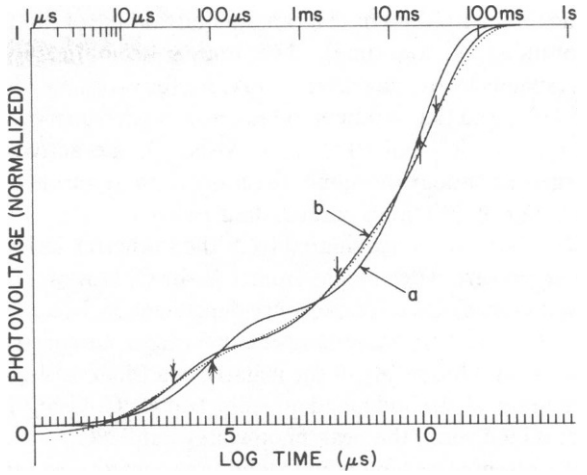

FIGURE 2 The results of nonlinear least-squares fitting are shown. The dotted curve is the data shown in Fig. 1. A five parameter (two exponentials plus offset) fit is shown by curve *a* with the time constants indicated by the up arrows. A seven parameter (three exponentials plus offset) fit is shown by curve *b* with the time constants indicated by the down arrows.

new functions (data arrays) are then formed: $S = V(t_2) - V(t_1)$ and $TM = (t_2 - t_1)/[\ln(t_2/t_1)]$, where t_1 = time interval (variable) after the initial excitation light pulse and $t_2 = 4\ t_1$. A simple analysis shows that a plot of S vs. TM exhibits a peak whenever $TM = \tau_i$. Using this simple correlator function, two peaks were found in S vs. TM corresponding to two time constants, τ_2 and τ_3. At 20°C, $\tau_2 = 33\ \mu s$ and $\tau_3 = 27$ ms. These time constants are indicated by the arrows in Fig. 1.

A nonlinear least-square fit program using the Marquardt algorithm (17) was also used to fit the data shown in Fig. 1. A five parameter two exponentials plus a constant) fit gave $\tau_2 = 100\ \mu s$ and $\tau_3 = 22$ ms with an amplitude ratio A_3/A_2 of 2.8. The resulting fit is shown as *a* in Fig. 1 and the relevant time constants are indicated by the up arrows. The five parameter fit really corresponds to three exponential components in the photovoltage but since $\tau_1 < 1\ \mu s$ the first component appears as a constant.

A seven parameter (three exponentials plus a constant) fit gave $\tau_2 = 38\ \mu s$, $\tau_3 = 2.4$ ms, and $\tau_4 = 33$ ms. The resulting fit is shown as *b* in Fig. 2 and the time constants are indicated by the down arrows. The relative amplitudes of each component in the fit are −0.02, 0.21, 0.22, and 0.60 so that $(A_3 + A_4)/A_2 = 3.9$. The seven parameter fit is considerably better than the five parameter one. The time constants derived from the correlation filter technique agree reasonably well with τ_2 and τ_4 from the seven parameter fit. For simplicity, the remainder of this paper will treat the photoresponse as though it were a five parameter curve. The correlation filter technique will be used to derive the time constants and the photovoltage vs. log time plots to determine the amplitudes of the corresponding exponentials. A more detailed analysis of the data using nonlinear least squares will be presented elsewhere.

Fig. 3 shows a family of photovoltage vs. log time isotherms. As in Fig. 1 each curve is a composite of 16,000 points taken at 0.5 μs/point and 16,000 points taken at from 5 μs/point to 200 μs point depending on the temperature. The intersection of the horizontal lines k to l and m to n with the isotherms agree well with the time constants derived using the correlation filter technique (arrows).

The slope of a log τ vs. $1/T$ (°K^{-1}) plot is commonly used to derive an activation energy for a thermally activated process. At these elevated temperatures $\delta(1/T)$ is $\cong \delta T/(T^2)$. Therefore, the activation energy can be directly estimated from the width between the extreme isotherms

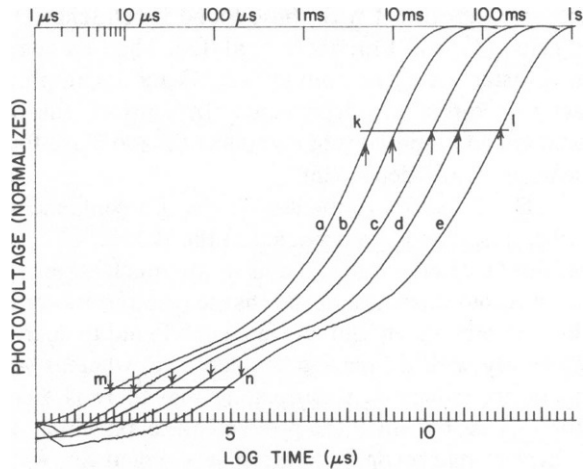

FIGURE 3 A family of photovoltage vs. log time isotherms ranging from 1 to 40°C is shown. The arrows indicate time constants found using the correlation filter techniques described in the text. The barrier heights corresponding to events 2 and 3 are calculated from the horizontal lines k to l and m to n and yield the activation energies $\Delta_2 = 55$ kJ/mol and $\Delta_3 = 62$ kJ/mol. (*a*) 40°C; (*b*) 30°C; (*c*) 20°C; (*d*) 10°C; (*e*) 1°C.

of the lines k to l and m to n (another advantage of plotting amplitudes vs. log time). The line m to n in Fig. 3 corresponds to an activation energy, Δ_2, for τ_2 of 55 kJ/mol (0.57 eV) and that of line k to l to an activation energy, Δ_3, for τ_3 of 62 kJ/mol (0.65 eV). Although the activation energies are about the same, the absolute magnitude of τ_3 is a factor of 800 times greater than τ_2.

The ratio A_3/A_2 calculated from the isotherms in Fig. 3 is temperature independent from 1 to 40°C. However, the peak photovoltage is temperature dependent and decreases by ~40% over the same temperature range. In constrast, the peak amplitude, A_1, of the negative transient was found to be temperature independent from 1 to 40°C. Using Fig. 1, A_1 is 0.04 times the peak photovoltage at 20°C.

An attempt was made to extend the temperature range to −20°C by using a bathing solution of 40% ethylene glycol, 100 mM NaCl, 5 mM $CaCl_2$, and 5 mM pipes buffered to pH 7. However, the presence of ethylene glycol increased τ_3 by a factor of ~2. Ethylene glycol had no measurable effect on τ_2. The rise time of the negative transient was faster than 1 μs even at −20°C. A bathing solution of 67% glycerol and salts had a similar effect (except that τ_3 was increased by even a larger factor). These results will be presented in detail elsewhere.

DISCUSSION

The results presented above fit the general framework established in the Introduction. A flash of light produces a very fast ($\tau < 1$ μs) negative photovoltage followed by a fast (microsecond) development of a positive potential that is followed finally by a slow (millisecond) rise to the peak photopotential. The overall temporal behavior of the photovoltage can be roughly characterized by the sum of three (exponential components (1, 2, and 3 of Fig. 1). The values of the time constants τ_2 and τ_3 measured in this work are in reasonable agreement with those found by Drachev et al. (6), Trissl (4), and Ehrenberg et al. (3). The first component is faster than 1 μs even at −20°C and its amplitude shows no temperature dependence. In contrast, the time constants and amplitudes of component 2 and 3 are found to be temperature dependent.

As mentioned above the amplitude of a component of the photoresponse is proportional to the product of charge times displacement. Since A_2 and A_3 are much larger than A_1 they account for most of the charge (proton) movement within the protein. A_2 and A_3 were each found to decrease significantly with decreasing temperature, whereas A_1 is temperature independent suggesting that there is a competing process by which the protein can relax, which does not involve macroscopic charge displacement across the protein. The implication is that the number of protons pumped per BR photocycling is temperature dependent. In contrast, A_3/A_2 was found not be temperature dependent, which supports the notion that this ratio is equal to $\delta x_3/\delta x_2$. Taking $A_3/A_2 = 3$ and assuming that the thickness of the membrane is 45 Å gives $\delta x_2 = 11$ Å and $\delta x_3 = 34$ Å. Similarly using the value for A_1 given above and assuming $q = e$ gives $\delta x_1 = 1.8$ Å. This value is only an estimate for δx_1 since first of all A_2 and A_3 are temperature dependent and second q may be some multiple of e for events 2 and 3.

The barrier heights Δ_2 and Δ_3 derived from the temperature dependence of the time constants are nearly equal even though the time constants are quite different. The near equality of Δ_2 and Δ_3 indicates that the passive proton channels (proton wires) involved in 1 and 2 are similar. The large difference in the time constants τ_2 and τ_3 could be explained by assuming a thermally activated stochastic process where the attempt frequency in event 2 is much higher than that in 3. The barrier heights derived from the temperature dependence of the time constants fall within limits suggested by theoretical studies of charge motion through β sheet (18) or along hydrogen bonded chains (12, 19). Studies with pH indicator dyes show that at pH 7 release precedes uptake and release is the faster process (20). Thus the active site lies closest to the extracellular surface rather than the cytoplasmic surface, whereas the reverse is the kinetically favored position for hydrogen-bonded chains (12).

The temperature independence of the amplitude A_1 shows that it is different from the events 2 and 3. Furthermore, results published by Trissl (14) indicate that τ_1 is <2 ns. It seems likely, therefore, that event 1 is not a thermally driven process but rather a photodriven charge displacement associated with an active (injector) site (12) or with the *trans-cis* isomerization of the chromophore. The recent time-resolved resonance Raman spectroscopy work of Hsieh et al. (21) suggests that the *trans-cis* isomerization of the chromophore takes place in <40 ps.

Several investigators have attempted to establish a direct time correlation between charge displacement within the protein and the photoreaction cycle (3, 7, 10, 11). The magnitudes of the decay times τ_1 and τ_2 are consistent with the general temporal behavior of the photoreaction cycle although significant discrepancies have been reported (6). The photoreaction cycle also exhibits a complicated pattern involving several intermediates and branching pathways (22), so that either the photovoltage has a complicated fine structure that has yet to be resolved or it is only loosely correlated with the photoreaction cycle. We have begun work to correlate the photoinduced charge displacements within the membrane to both the photoreaction cycle and to proton release and uptake in the surrounding medium.

This work was supported by the National Institutes of Health grant GM 26669.

The technical help of Y. H. Hifeda and D. C. Mitchell is greatly appreciated.

Received for publication 6 August 1984 and in final form 11 January 1985.

REFERENCES

1. Stoeckenius, W. R., and H. Loziar. 1979. Bacteriorhodopsin and the purple membrane of *Halobacteria*. *Biochim. Biophys. Acta.* 505:215–278.
2. Eisenback, M., and S. R. Caplan. 1979. The light-driven proton pump of *Halobacterium halobium*: mechanism and function. *Curr. Top. Membr. Transp.* 12:166–248.
3. Ehrenberg, B., Z. Meiri, and L. M. Loew. 1984. A microsecond kinetic study of the photogenerated membrane potential of bacteriorhodopsin with a fast responding dye. *Photochem. Photobiol.* 39:199–205.
4. Trissl, H. W. 1983. Charge displacements in purple membranes adsorbed to a heptane/water interface. Evidence for a primary charge separation in bacteriorhodopsin. *Biochim. Biophys. Acta.* 723:327–331.
5. Rayfield, G. W. 1983. Events in proton pumping by bacteriorhodopsin. *Biophys. J.* 41:109–117.
6. Drachev, L. A., A. D. Kaulen, L. V. Khitrina, and V. P. Skulachev. 1981. Fast stages of photoelectric processes in biological membranes. *Eur. J. Biochem.* 117:461–470.
7. Fahr, A., P. Lauger, and E. Bamberg. 1981. Photocurrent kinetics of purple-membrane sheets bound to planar bilayer membranes. *J. Membr. Biol.* 60:51–62.
8. Huebner, J. S., R. T. Arrieta, I. C. Arrieta, and P. M. Pachori. 1984. Photo-electric effects in bilayer membranes: electrometers and voltage clamps compared. *Photochem. Photobiol.* 39:191–198.
9. Rayfield, G. W. 1982. Kinetics of the light-driven proton movement in model membranes containing bacteriorhodopsin. *Biophys. J.* 38:79–84.
10. Varo, G., and L. Keszthelyi. 1983. Photoelectric signals from dried oriented purple membranes of *Halobacterium halobium*. *Biophys. J.* 43:47–51.
11. Keszthelyi, L., and P. Ormos. 1980. Electric signals associated with the photocycle of bacteriorhodopsin. *FEBS* (*Fed. Eur. Biochem. Soc.*). *Lett.* 109:189–193.
12. Nagle, J. F., and S. Tristram-Nagle. 1984. Elements of proton pump models. *In* Information and Energy Transduction in Biological Membranes. C. L. Bolis and E. J. M. Helmreich, editors. A. R. Liss, Inc., New York. 103–104.
13. Becher, B. M., and J. Y. Cassium. 1975. Improved isolation procedures for the purple membranes of *Halobacterium halobium*. *Prep. Biochem.* 5:161–178.
14. Trissl, H. W. 1980. Novel capacitance electrode with a wide frequency range for measurements of flash-induced changes of interface potential at the oil-water interface. *Biochim. Biophys. Acta.* 595:82–95.
15. Nagle, J. F. 1981. Upon the optimal graphical representation of flash data from photochemical systems obeying first order kinetics. *Photochem. Photobiol.* 33:937–939.
16. Crowell, C. R., and Alipanahi, S. 1980. Transient distortion and nTh order filtering in deep level transient spectroscopy (D^nLTS). *Solid State Electronics.* 24:25–36.
17. Bevington, P. R. 1969. Data Reduction and Error Analysis for the Physical Sciences. McGraw-Hill, Inc., New York. 235–239.
18. Glaeser, R. M., and B. K. Jap. 1984. The "born energy" problem in bacteriorhodopsin. *Biophys. J.* 45:95–97.
19. Scheiner, S., and E. A. Hillenbrand. 1984. Analysis of proton translocation through hydrogen-bonded chains using molecular orbital methods. *Proc. 2nd Int. Conf. Water Ions Biol. Syst.* In press.
20. Lozier, H. R., W. Niederberger, R. A. Bogomolni, S. B. Hwang, and W. Stoeckenius. 1976. Kinetics and stoichiometry of light-induced proton release and uptake from purple membrane fragments. *Halobacterium halobium* cell envelopes, and phospholipid vesicles containing oriented purple membrane. *Biochim. Biophys. Acta.* 440:545–555.
21. Hsieh, C.-L., M. A. El-Sayed, M. Nicol, M. Nagumo, and J.-H. Lee. 1983. Time-resolved resonance Raman spectroscopy of the bacteriorhodopsin photocycle on the picosecond and nanosecond time scales. *Photochem. Photobiol.* 38:83–94.
22. Renard, M., P. Thirion, and M. Delmelle. 1983. Photoacoustic spectroscopy of bacteriorhodopsin photocycle. *Biophys. J.* 44:211–218.